The best peg and socket joint

Zhibin Zou Weifu Wang

Abstract

In this work, we study how to find the best design for insertion based joints, i.e. the best design for a peg-and-hole problem, to ensure the ease of insertion subject to manufacturing errors, and the stability after insertion under external disturbances. The design relies on discretization of both the insertion process and the stability analysis. Through sequence of numerical optimizations on the discrete states and their transitions, we find the best 2D design first, then project to 3D for the block design. The 2D design results are compared both theoretically and through experiments.

1 Introduction

Automated assembly is one of the classic tasks in the robotics community, and has been explored using different approaches. The capability to form large stable structures using small blocks can push the boundary of the automation in field robotics, especially in construction.

In this work, we focus on the design aspect of a particular assembly approach: assembly large structures using uniform blocks that lock each other with passive joints, i.e. joineries. Using the joints to align the building blocks, and relying on the geometries of the blocks to support the assembled structure, this *joinery-based* assembly can lead to particular simple assembly routine for robots, yet result in interesting structures.

We will focus on insertion based joints, which are very similar to the subjects of the classical peg-and-hole problem. Assembly using insertion based joints relies on the different orientations of the insertion joints, i.e., different assembly directions, to interlocks the blocks and secure the assembled structure. Moving beyond theoretical analysis, when manufacturing error and manipulation error can both exist, how can peg and socket be designed so that the insertion is easy for assembly, possibly error-reducing, while after the insertion the peg remains *stable* under external disturbances?

In this work, we measure the quality of the design from two perspectives: the chance of success for insertion, and the stability of the peg in the socket after insertion. The analysis for a single criteria, especially for stability, has been studied before, mostly as an analysis tool. This work proposes to use both criteria in the derivation of the design, to optimize the design for both the execution (insertion) and the structure stability.

Our analyze builds upon the assumption of point-edge (surface) contact between the peg and the socket, rather than the surface-surface contact. In the previous work, where we designed for surface contacts between pegs and sockets, the manufacturing error often destroys the assumption, and lead to unpredictable behaviors of the blocks both during and after the insertion. The main cause of the unpredictable behaviors is the unknown actual contact locations between the peg and the socket. Therefore, under the assumption of the point-surface contact, even when error can exist, as long as the error is upper bounded, a point-surface contact design can always result in known contact locations between peg and the socket.

The design process is a numerical process relying on sequences of optimizations. Due to the numerical instability, even under the assumption

of linear edges and surfaces, the global optimal solution can be difficult to find. The detail of the design process is presented in Section 3. We analyze the insertion process and the stability after insertion separately, and using each process to find the *gradient* information of how design changes can affect the insertion and stability respectively. Using the derived information, improved design will be found and analyzed again until limited improvements can be made.

The design process also starts from the 2D plane, finding the *best* 2D design for a pair of peg and socket, and then project to 3D. The current 3D design consists of the same 2D design laying on two perpendicular planes. There also exist other 3D projection approaches, which we will study and compare in the future work.

2 Related work

[1] focus on misalignment situation and gives kinematic and geometric methods to model the contact of *"peg on hole"*, respectively.

[2] imitate human's contact motion by passive compliance and reinforce learning.

Linearizing motion around an initial configuration allows study of systems of blocks with many thousand degrees of freedom; our approach draws inspiration from early work on *manipulability ellipsoids* [3]–[6], in which directions of motion of the end effector of a robot arm are analyzed at a particular configuration by examining eigenvectors of the Jacobian matrix. Work by Berenson also provides analysis and approximations of Jacobians for truly flexible cloth or string [7]. Linear grasp analysis techniques also serve as inspiration. In the 19th century, Reuleaux [8] derived a geometric method to find the free motion of an object in contact with frictionless fingers. Mishra, Schwartz, and Sharir's seminal work on the minimum number and sufficient placement of fingers to immobilize an object [9] analyzes polyhedral constraints in twist and wrench spaces.

In contrast to manipulability and grasping problems, the blocks which we consider are only loosely connected. Caging grasps [10]–[16] study how robot hands may loosely capture an object; the present paper studies motion of structures in which either pairs of blocks or combinations of many blocks may cage each other. Direct construction of configuration spaces of pairs of blocks has a long history; Sacks *et al.* [17] provides a recent approach, and gives a much higher-fidelity representation of the free motions of small numbers of blocks than our edge/point distance function model. Eckstein *et al.* [18] analyze how forgiving a connector design is using an explicit approximation of the configuration space of the joint.

The Carpenter's Rule Theorem states that any open polygonal chain (a planar revolute robot arm) can be reconfigured arbitrarily without self-intersection [19]; the proof uses *expansive motions* that cause points and edges to separate from one another. The motions in the present paper allow points and edges to approach one another, while balancing the rates so as to optimize net motion in some direction. The distance constraints are similar to those used in Linear Complementarity Problem (LCP) formulations of dynamics [20], [21], which have been used both for rigid body simulation and design for manipulation [22].

Tolerance analysis of mechanical assemblies is utilized in mechanical engineering to determine how frequently small manufacturing errors in the component parts of an assembly will result in unacceptable deviations in the final assembly [23]. The Direct Linearization Method [24] linearizes the homogeneous transformation matrices describing the kinematics of an assembly, and applies statistical techniques to determine what percentage of assemblies are able to be assembled.

3 Joint design process

In this section, we present the details of the design process. The analysis and the design process

is derived under the assumption of the existence of manufacturing error. For simplicity of analysis, the error is assumed to be uniform, and was only attached to the socket while the peg is *perfect*. Though the analysis of the peg and the socket are both considered in isolation, both the peg and the socket are part of a block, which is of limited size. Therefore, the size of the peg and the socket are limited with respect to the block.

The design process for insertion and the stability after insertion are analyzed separately. In the insertion process, the main goal is for the peg to be fully inserted into the socket, regardless of the initial configuration or the intermediate stages the insertion has to go through. The initial insertion configuration of the peg is assumed to be within a bounded error of the perfect insertion location and orientation, simulating the sensing error and grasping error during assembly. The success of transition between different stages is the key to reaching the final inserted configuration, which we refer as a *sink*. The analysis of the insertion stage focus on ensuring the success of these transitions.

After the insertion, the peg may move within the socket under external disturbance, if the manufacturing error exists. As the relative translation of the peg within the socket is unavoidable, the main goal for the peg stability is to achieve the minimum possible rotation within the socket. A design change that reduces such rotation is considered an improvement, and finding such changes is the goal for the stability analysis.

As the design of the joint consists of two parts, the peg and the socket, we will consider the change of one component of the joint only for each process. In the insertion stage, we will treat the peg as a fixed design, and study how the socket can be changed to maintain the success of insertion transitions and possibly improve the ease of transition. In the stability analysis after the insertion, we will treat the socket as a fixed design, and change the peg shape, i.e. the contact locations between the peg and socket to improve the stability. Then, through the iterations of the insertion and stability analysis, we can find the *best* design that is beneficial to insertion and stability.

3.1 Mode of contacts and transitions

During the insertion, the peg may contact the socket along different edges at different locations. Maintaining the contacts at different edges requires different set of constraints. Therefore, to ensure the success of insertion, there are different sets of constraints one needs to maintain, depending on the *stage* of insertion. This makes the straight optimization of joint design difficult to model.

On the other hand, the different sets of constraints can be considered separately, if we discretize the insertion process. We define *Mode of Contacts* as a collection of point-edge pairs that are in contact, and to each point-edge pair that is in contact as a *Contact Pair*, denoted as $CP(i,j) = \{p_i, e_j\}$. We use p_i to denote the ith point on the peg following a counter-clockwise order, and e_j to denote the jth edge on the socket in the counter-clockwise order. We also denote the Mode of Contact as $MoC(k) = \{CP(a,b), CP(c,d), \ldots\}$. Then, the entire insertion process can be described as a directed graph when the insertion is guided by a known force.

In this paper, we only consider the Contact-Pair as the pair containing a point on a peg and an edge on the socket. For simplicity, the points on the peg can be joined by different designs (curves) to avoid any contact between the socket edges other than the bounded number of designed contact points. In addition, a point on the peg contacting two adjacent edges on the socket, i.e., a point-point contact, can be viewed as two contact pairs. Therefore, the Contact-Pair defined above is the fundamental unit for analyzing the Mode of Contact in the peg-socket relation.

We will first find the set of all valid Mode of Contacts (MoCs). In order for a Mode of Contact to be valid, all the containing Contact Pairs need to be valid for the given peg and socket, and

a valid configuration must exist to allow the set of Contact Pairs to co-exist. We adapted a bottom up approach to find the valid MoCs: identifying all valid Contact Pairs (CPs), and find all combinations of CPs to form potential valid MoCs; for each of the candidate valid MoC, we test if there exist a valid configuration allowing the set of CPs co-exist.

The MoCs along cannot fully describe the insertion process, as the insertion process also involves the transition between different modes. To find out whether a transition between two Mode of Contact under a given force is possible, we can find the acceleration direction under the insertion force, and the location of the different CPs between the two modes. If the acceleration / moving direction can lead to the contact or the removal of the corresponding point-edge pairs, then the transition is valid, otherwise not.

There is a huge number of possible transitions among all valid MoCs. For simplicity, we can view a potential transition between arbitrary two modes as a sequence of transitions between two *adjacent modes*. Given $MoC(i)$ and $MoC(j)$, if the difference between the two MoCs is d Contact Pairs $CP_k(a,b), 1 \leq k \leq d$, then we refer these two MoCs as *d-neighbors*. We can show that arbitrary *valid* transition between two MoCs during insertion can be decomposed to either a sequence of transitions between 1-neighbor MoCs, or a special transition between k-neighbors where k can be uniquely computed for given peg and socket, and there can only exist a bounded number of special transitions. In addition, add a special MoC with no contact pairs.

We therefore can define a directed graph $G = (V, E)$, where V is the set of valid MoCs, and E are the valid transitions between neighbor modes or among special modes. We refer this graph as the Contact Mode Transition (CMT) graph. Then, for each vertex on the graph, the set of constraints describing the relation between peg and socket is of fixed number.

To simulate the sensing error during automated assembly, we introduce a Δx and a $\Delta\phi$ during insertion process. The two values denote the maximal offset along x axis and the maximal rotation allowed at the beginning of the insertion, which is bounded by the precision of the sensing technology. Under such initial error, we would like the designed peg to still be able to be inserted into the socket. One of the necessary condition for the success of insertion is the peg not contacting any edge outside the socket, which we refer to as the *capture* of the peg. In the remaining section of paper, for simplicity, we connected contact points on the peg with straight edges, but the actual design may require these connection to be curved to avoid undesigned contacts.

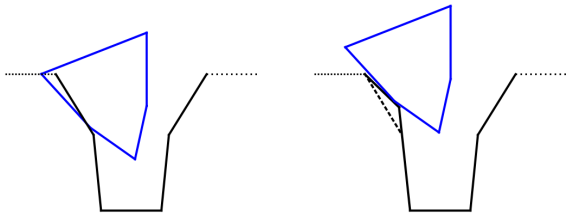

(a) The peg is not captured by the socket. (b) The peg is captured by the socket.

Figure 1: An example of peg not captured by the socket, and how the socket can be changed to guarantee the capture.

Figure 1a shows an example of the peg not captured by the socket. In the given example, p_1 contacts the outside the socket during insertion, which can prevent further insertion. However, by rotating the top-left edge of the socket, the peg can be captured in Figure 1b with same Δx and $\Delta\phi$. After the peg is captured by the socket, we can derive its CMT graph.

Define a *sink* on the CMT graph as a vertex that either has only in coming edges, or has outgoing edges and incoming edges with another *sink*. A insertion process can be considered successful only if the CMT graph has sinks, but the inverse statement is not true, as some sinks are not desired. For example, a CMT graph for a

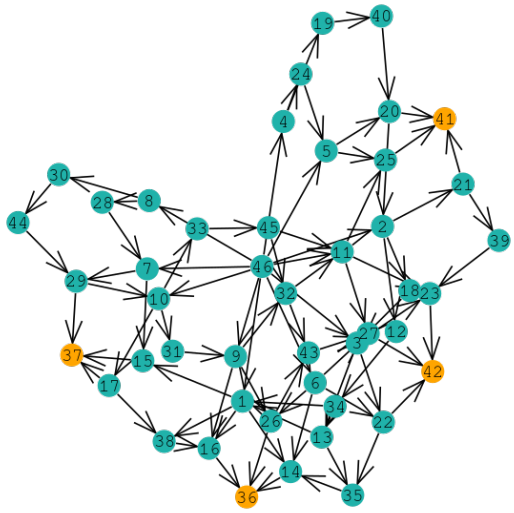

Figure 2: The insertion graph of a five-point and five-edge peg-socket joint.

five-edge socket and a five-point peg is shown in Figure 2, four sinks are identified, and are shown in Figure 3. The sinks shown in Figure 3b and 3c are not desired, as the peg is not fully inserted and by definition the peg cannot get out of the MoC under the insertion force.

3.2 Stability after insertion

Another important criteria for a good peg-socket design is how stable the peg will be in the socket after insertion, under external disturbances and subject to manufacturing error. Under the assumption of an uniform error, the translation of the peg inside the socket after insertion is unavoidable regardless of the design, but the possible rotations can be reduced by changing the designs.

Intuitively, given the same amount of error ϵ between the peg and the socket, the longer the peg is, the less rotation is possible after insertion. However, as the peg and the socket are both part of a block, which has bounded size, we have to assume the maximum depth of the socket is bounded. The question then becomes, how will the different designs of peg and socket reduce possible rotations after insertion?

We again discretize the possible motions of the peg in the socket after insertion based on different Mode of Contacts (MoCs). The key observation is that, there exist a partial order of all the valid MoCs, based on the possible rotations of the peg. For example, consider the two Modes of Contact shown in Figure 3a and 3b, the MoC shown in Figure 3b will always have a larger rotation compared to the MoC shown in Figure 3a. Based on this derived partial order, we therefore only need to analyze the MoCs with the highest order, i.e. the largest possible rotation. In addition, we do not want to consider the scenarios where the peg has moved away from the socket, thus we will add a *virtual cap* near the entrance of the socket.

Let us define a contact point on the peg as a function of s, the length along a given socket edge. Then, the design of the peg becomes a collection of pairs, (i, s), where i denotes the designed contacting edge for the given contact point, and s is the distance along the edge following the counter-clockwise direction. This definition is only valid when no error is introduced, i.e. the design for the perfect peg and socket.

Based on the previously derived partial order, we analyze the MoCs with the highest order, and study how does the change of s can affect the rotation angle of the peg inside the socket after insertion. Then, we can effectively find a direction (*gradient*) of contact-point (on the peg) motion that will reduce the possible rotation. Paired with the socket-edge rotation direction that can preserve (or break) the insertion transition, we can derive the following design procedure to find the *best* design for the joint.

3.3 Design procedure

Combining the analysis for the peg and the socket design, we propose the following design procedure.

1. Input: an initial (arbitrary) design of m edges (socket) and n contact points (peg);

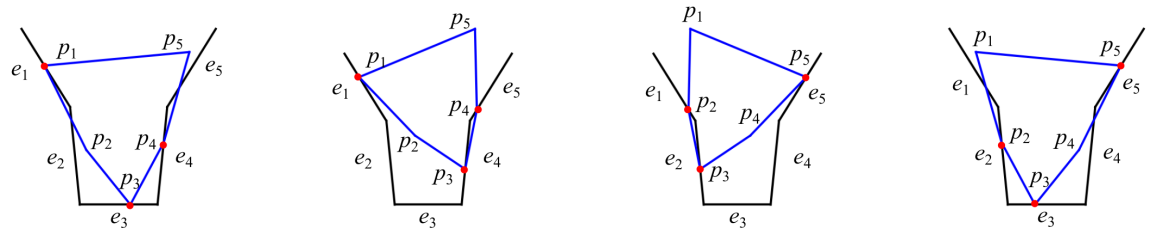

(a) Sink 1. $MoC(36)$ with $CP(1,1)$, $CP(3,3)$ and $CP(4,4)$.

(b) Sink 2. $MoC(36)$ with $CP(1,1)$, $CP(3,4)$ and $CP(4,5)$.

(c) Sink 3. $MoC(41)$ with $CP(2,1)$, $CP(3,2)$ and $CP(5,5)$.

(d) Sink 4. $MoC(42)$ with $CP(2,2)$, $CP(3,3)$ and $CP(5,5)$.

Figure 3: Sinks of an insertion CMT graph for joint with five-point peg and five-edge socket.

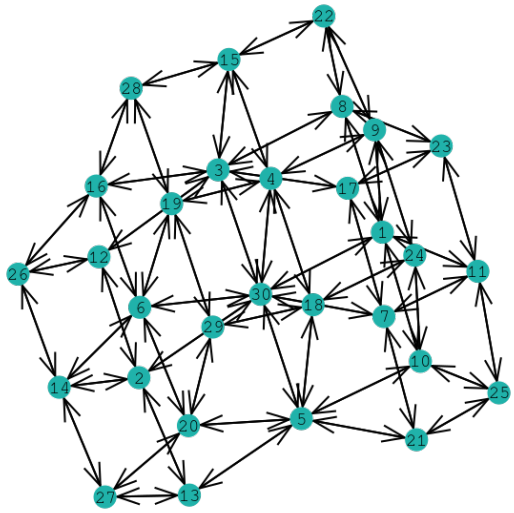

Figure 4: The CMT graph of the peg in socket.

friction coefficient μ, and a force magnitude $|F|$;

2. Find all possible CPs and MoCs for insertion, generate the CMT graph for insertion (G_I);
3. Identify sinks, if undesired sinks exist, find edges moving directions that will remove them as sink, and change the design, until no undesired sink exist on the CMT graph;
4. For each transition, identify the direction of socket edge rotation direction that will break the transition;
5. Generate the CMT graph for stability G_S, generate the partial order for nodes;
6. For each of the nodes with the highest order, find the contact-point gradient for reducing rotation;
7. While G_I remains the same and the rotation angle reduction $\Delta\phi$ is larger than δ, the change of the edge angle or the change in s, iteratively move the points and rotate the edges to reduce the possible rotation after insertion; output the final design;
8. If the G_I is changed, compute the new insertion CMT graph G_I', see if the new graph contains undesired sinks, if no, repeat the process for G_I' starting from step 4;

Using the procedure described above, with $m = 5$ and $n = 5$, we can find the following design show in Figure 7a. The blue shape is the initial input, while the red shape is the peg design output by the procedure above. In the process, we maintained an uniform error of ϵ on the socket.

The best design for the joint overall may not share the m and n imagined by the user. Therefore, the procedure above should be put inside a loop that test different m and n. However, we do not need to test m and n as two independent variables, as n cannot be too different from m. If $|m - n| \geq 2$, then, there exist either two or more edges on the socket with no active contact

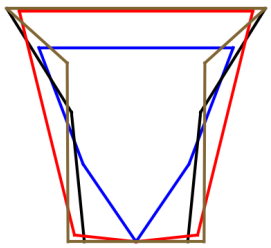

Figure 5: Optimized peg-socket joint design (red and brown) and given peg-socket joint (blue and black) with five peg points and five socket edge.

points in the inserted configuration, or there exist two or more contact points on the peg that contacts along the same edge. The non-contact edge is redundant as they do not provide additional constraint on the rotation, and the colinear contact points are redundant as one of the contact point will provide no constraint when rotated, leaving some contact points with no effect at all. Therefore, we only need to consider the case where $|m-n|<2$. Also, as six contacts are sufficient to immobilize arbitrary planar object, we only need to test m up to 6, and no less than 3. Therefore, the complete design procedure will be the above presented procedure nested inside a loop over m and n.

When the number of edges on the socket exceed four, the shape of the socket can be either convex or concave. Naively, the convex design allows fast initial insertion, and will fine-tune the orientation in the later stage of insertion; while the concave shape will provide a slow initial insertion process, but quickly aligns peg towards the targeted orientation after the peg is mostly inside the socket. The fast initial insertion, however, may cause one or more of the contact point on the peg to contact edges outside the socket, i.e. fail to capture. In fact, it can be proven that based on the above capture definition, in order to capture the peg, the convex design permits much smaller initial Δx and $\Delta\phi$.

Lemma 1. *Given a Δx and $\Delta\phi$, the initial offset along x axis and orientation for the peg. Denote θ_{ei} ($|\theta_{ei}| \le \pi/2$) as the angle between e_i and horizontal line, θ_{pi} ($|\theta_{pi}| \le \pi/2$) as the angle between the line go through p_i and p_{i+1} and horizontal line. If $\exists \Delta x > 0$ let a point of the peg (p_1) outside the edge of the socket near the entrance (e_1), θ_{e1} needs to be no larger than $\theta_{p1} - \Delta\phi$ to induce the capture of peg with point-edge contacts with socket.*

Proof. Assume $\theta_{e1} > \theta_{p1} - \Delta\phi$.

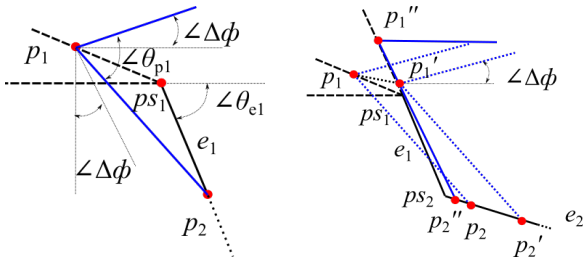

(a) p_2 contact e_1 first. (b) p_2 contact e_2 first.

Figure 6: Induce capture for $\theta_{e1} > \theta_{p1} - \Delta\phi$.

- Figure 6a shows the case p_2 contact e_1 first. Easily have the signed distance between p_1 and e_1 is negative. Denote the start point of e_1 as ps_1. To ensure the signed distance become non-negative before contacting outside the socket, the moving direction of p_1 should no less than $p_1 \to ps_1$.

  1. If $\theta_{e1} \le 2\pi - \Delta\phi$, p_1 would move along $ps_1 \to p_2$, which is less than $p_1 \to ps_1$. Contradiction.
  2. If $\theta_{e1} > 2\pi - \Delta\phi$, p_1 would move along with $\Delta\phi$. Since $\theta_{p1} \le \pi/2$, $\Delta\phi$ is no larger than the direction $p_1 \to ps_1$, thus less than $p_1 \to ps_1$. Contradiction.

  Thus, if $\theta_{e1} > \theta_{p1} - \Delta\phi$ and p_2 contact e_1 first, p_1 would contact outside the socket during insertion.

- For the case p_2 contact e_2 first.

1. If the signed distance between p_1 and e_1 is negative, as analyzed above, the direction of $ps_2 \rightarrow p_2$ should no less than $p_1 \rightarrow ps_1$ to allow p_1 captured, where ps_2 is the start point of e_2.

   As shown in Figure 6b, if $ps_2 \rightarrow p_2$ no less than $p_1 \rightarrow ps_1$, the signed distance between p_1 and e_1 can become zero during insertion e.g., p_1 and p_2 moved to p_1' and p_2', where p_1' is on or above ps_1. Then, let $d\theta = 0$, p_1' and p_2' would move to p_1'' and p_2''. We can see the p_1'' must on the extension cord of e_1, which means $s < 0$. Contradiction.

2. If the signed distance between p_1 and e_1 is not negative. For $\theta_{e2} < \theta_{e1}$, move p_1 along $p_2 \rightarrow ps_2$ to make signed distance zero. Then do the same with above, we can also get $s < 0$. For $\theta_{e2} \geq \theta_{e1}$, e.g., collinear and concave cases, which means the singed distance between p_2 and e_1 is 0 or negative. To make the signed distance between p_1 and e_1 not negative, the direction of $p_2 \rightarrow p_1$ should maintain or increase signed distance to e_1, which means $\theta_{e1} \leq \theta_{p1} - \Delta\phi$. Contradiction.

If the p_2 contact e_2 first, to induce the p_1 captured, there must be contradictions for $0 \leq s \leq 1$ or $\theta_{e1} > \theta_{p1} - \Delta\phi$.

□

Based on the above Lemma, the entrance of the socket needs to be gentle to induce capture, i.e. correcting the displacement along x axis for the peg, before aligning the orientation. In initialization, as the point of the peg defined on the edge of the socket by s, if $\theta_{e1} < \theta_{p1}$, the signed distance between p_2 and e_1 must be negative. However, if the socket were to be of convex shape, the signed distance between all points of the peg and all edges of the socket should be non-negative. Therefore, for the convex socket, we must have $\theta_{e1} \geq \theta_{p1}$, then $\theta_{e1} > \theta_{p1} - \Delta\phi$ for $\Delta\phi > 0$. It means for the convex socket, we can never induce the peg captured as long as there is a point of the peg outside the socket with $\forall\Delta\phi > 0$. Concave shape sockets, therefore, is much more suitable for insertion. Which means we can actually cut down the loop for m, only considering cases where $m > 4$.

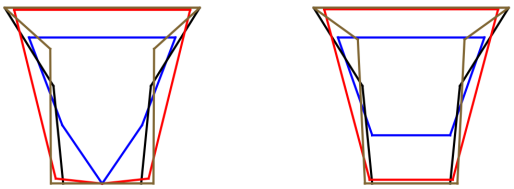

(a) The initial design (blue and black) and optimized design (red and brown) for the 5-5 joint.

(b) The initial design (blue and black) and optimized design (red and brown) for the 4-5 joint.

Figure 7: The initial design and optimized design for two joints.

In the case of $m = 5$, we find the difference of the possible rotation before and after the optimization for the design, and see a big improvement for the possible rotation, in radian.

Table 1: The possible rotations for the joints with $m = 5$.

$n - m$	**Max rotation**	**Max rotation**
4-5 joint	0.1764	0.0383
5-5 joint	0.1878	0.0372

As shown in Table 1, the stability of both joints has been increased after optimizing. However, the difference of stability between the two optimized joints are very small.

4 Conclusion and future work

In this paper, we have analyzed the ideal peg and socket joint in 2-D plane with respect to the insertion and stability. To analyze the constraint

for insertion and the gradient of the stability, we have discretized the insertion process and the "rocking" process for the peg in the socket. Besides, we have proved the concave joint is better than convex joint with respect to capture. The designed algorithm can optimize and compare the peg and socket joint so as to get best peg and socket joint design. In the future, we would extend the 2-D joint design to 3-D, then explore the assembling for the best joint block by the manipulator.

References

[1] H. Bruyninckx, S. Dutre, and J. De Schutter, "Peg-on-hole: A model based solution to peg and hole alignment," in *Proceedings of 1995 IEEE InternationalComparative Peg-in-Hole Testing of a Force-Based Manipulation Controlled Robotic Hand Conference on Robotics and Automation*, IEEE, vol. 2, 1995, pp. 1919–1924.

[2] S.-k. Yun, "Compliant manipulation for peg-in-hole: Is passive compliance a key to learn contact motion?" In *2008 IEEE International Conference on Robotics and Automation*, IEEE, 2008, pp. 1647–1652.

[3] P. Chiacchio, S. Chiaverini, L. Sciavicco, and B. Siciliano, "Global task space manipulability ellipsoids for multiple-arm systems," *IEEE Trans. Robot. Autom.*, vol. 7, no. 5, pp. 678–685, 1991.

[4] F. C. Park and J. W. Kim, "Manipulability and singularity analysis of multiple robot systems: A geometric approach," in *Proc. ICRA*, 1998, pp. 1032–1037.

[5] S. Kim, "Adjustable manipulability of closed-chain mechanisms through joint freezing and joint unactuation," in *Proc. ICRA*, 1998, pp. 2627–2632.

[6] A. Bicchi and D. Prattichizzo, "Manipulability of cooperating robots with unactuated joints and closed-chain mechanisms," *IEEE Trans. Robot. Autom.*, vol. 16, no. 4, pp. 336–345, 2006.

[7] D. Berenson, "Manipulation of deformable objects without modeling and simulating deformation," in *Proc. IROS*, 2013, pp. 4525–4532.

[8] F. Reuleaux, *The kinematics of machinery*. 1876.

[9] B. Mishra, J. T. Schwartz, and M. Sharir, "On the existence and synthesis of multifinger positive grips," *Algorithmica*, vol. 2, pp. 541–558, 1987.

[10] A. Rodriguez, M. T. Mason, and S. Ferry, "From caging to grasping," *Int. J. Robot. Res.*, vol. 31, no. 7, pp. 886–900, 2012.

[11] S. Makita and Y. Maeda, "3d multifingered caging: Basic formulation and planning," in *Proc. IROS*, 2008, pp. 2697–2702.

[12] M. Vahedi and A. F. van der Stappen, "Caging polygons with two and three fingers," *Int. J. Robot. Res.*, vol. 27, no. 11-12, pp. 1308–1324, 2008.

[13] J. Erickson, S. Thite, F. Rothganger, and J. Ponce, "Capturing a convex object with three discs," in *Proc. ICRA*, vol. 2, 2003, pp. 2242–2247.

[14] E. Rimon and A. Blake, "Caging 2d bodies by 1-parameter two-fingered gripping systems," in *Proc. ICRA*, 1996, pp. 1458–1464.

[15] T. F. Allen, J. W. Burdick, and E. Rimon, "Two-finger caging of polygonal objects using contact space search," *IEEE Trans. Robot.*, vol. 31, no. 5, pp. 1164–1179, 2015.

[16] S. Makita and W. Wan, "A survey of robotic caging and its applications," *Advanced Robotics*, vol. 31, no. 19-20, pp. 1071–1085, 2017.

[17] E. Sacks, N. Butt, and V. Milenkovic, "Robust free space construction for a polyhedron with planar motion," *Computer-Aided Design*, vol. 90, pp. 18–26, 2017.

[18] N. Eckenstein and M. Yim, "Modular robot connector area of acceptance from configuration space obstacles," in *Proc. IROS*, 2017, pp. 3550–3555.

[19] R. Connelly, E. D. Demaine, and G. Rote, "Straightening polygonal arcs and convexifying polygonal cycles," *Discrete and Computational Geometry*, vol. 30, no. 2, pp. 205–239, 2003.

[20] D. Stewart and J. Trinkle, "Dynamics, friction, and complementarity problems," in *Complementarity and Variational Problems*, M. Ferris and J. Pang, Eds., SIAM, 1997, pp. 425–439.

[21] J. Trinkle, J. Tzitzouris, and J. Pang, "Dynamic multi-rigid-body systems with concurrent distributed contacts: Theory and examples," *Philosophical Transactions: Mathematical, Physical, and Engineering Sciences*, A, vol. 359, no. 1789, pp. 2575–2593, Dec. 2001.

[22] D. Balkcom and J. C. Trinkle, "Computing wrench cones for planar rigid body contact tasks," vol. 21, no. 12, pp. 1053–1066, 2002.

[23] K. W. Chase and A. R. Parki nson, "A survey of research in the application of tolerance analysis to the design of mechanical assemblies," *Research in Engineering Design*, vol. 3, no. 1, pp. 23–37, 1991.

[24] K. W. Chase, J. Gao, S. P. Magleby, and C. D. Sorensen, "Including geometric feature variations in tolerance analysis of mechanical assemblies," *IIE Transactions*, vol. 28, no. 10, pp. 795–807, 1996.